



**HAL**  
open science

## **An Auxin-Mediated Shift toward Growth Isotropy Promotes Organ Formation at the Shoot Meristem in Arabidopsis**

Massimiliano Sassi, Olivier Ali, Frédéric Boudon, Gladys Cloarec, Ursula Abad, Coralie Cellier, Xu Chen, Benjamin Gilles, Pascale Milani, Jirí Friml,  
et al.

► **To cite this version:**

Massimiliano Sassi, Olivier Ali, Frédéric Boudon, Gladys Cloarec, Ursula Abad, et al.. An Auxin-Mediated Shift toward Growth Isotropy Promotes Organ Formation at the Shoot Meristem in Arabidopsis. *Current Biology - CB*, 2014, 24 (19), pp.2335-2342. 10.1016/j.cub.2014.08.036 . hal-01074821

**HAL Id: hal-01074821**

**<https://inria.hal.science/hal-01074821v1>**

Submitted on 7 Jan 2015

**HAL** is a multi-disciplinary open access archive for the deposit and dissemination of scientific research documents, whether they are published or not. The documents may come from teaching and research institutions in France or abroad, or from public or private research centers.

L'archive ouverte pluridisciplinaire **HAL**, est destinée au dépôt et à la diffusion de documents scientifiques de niveau recherche, publiés ou non, émanant des établissements d'enseignement et de recherche français ou étrangers, des laboratoires publics ou privés.

Copyright

# An Auxin-Mediated Shift toward Growth Isotropy Promotes Organ Formation at the Shoot Meristem in *Arabidopsis*

Massimiliano Sassi,<sup>1,\*</sup> Olivier Ali,<sup>1,2</sup> Frédéric Boudon,<sup>2</sup> Gladys Cloarec,<sup>1</sup> Ursula Abad,<sup>1</sup> Coralie Cellier,<sup>1</sup> Xu Chen,<sup>3,4</sup> Benjamin Gilles,<sup>5</sup> Pascale Milani,<sup>1,6</sup> Jirí Friml,<sup>3,4</sup> Teva Vernoux,<sup>1</sup> Christophe Godin,<sup>2</sup> Olivier Hamant,<sup>1,6</sup> and Jan Traas<sup>1,\*</sup>

<sup>1</sup>Laboratoire de Reproduction et Développement des Plantes, INRA, CNRS, ENS, UCB Lyon 1, 46 Allée d'Italie, 69364 Lyon Cedex 07, France

<sup>2</sup>CIRAD, INRIA, INRA, Virtual Plants INRIA Team, UMR AGAP, Avenue Agropolis, TA 108/02, 34398 Montpellier Cedex 5, France

<sup>3</sup>Department of Plant Systems Biology, Flanders Institute for Biotechnology (VIB), and Department of Plant Biotechnology and Bioinformatics, Ghent University, Technologiepark 927, 9052 Gent, Belgium

<sup>4</sup>Institute of Science and Technology Austria (IST Austria), Am Campus 1, 3400 Klosterneuburg, Austria

<sup>5</sup>Laboratoire d'Informatique, de Robotique et de Microlélectronique de Montpellier, CNRS, Université Montpellier 2, 34090 Montpellier, France

<sup>6</sup>Laboratoire Joliot Curie, CNRS, ENS Lyon, Université de Lyon, 46 Allée d'Italie, 69364 Lyon Cedex 07, France

## Summary

To control morphogenesis, molecular regulatory networks have to interfere with the mechanical properties of the individual cells of developing organs and tissues, but how this is achieved is not well known. We study this issue here in the shoot meristem of higher plants, a group of undifferentiated cells where complex changes in growth rates and directions lead to the continuous formation of new organs [1, 2]. Here, we show that the plant hormone auxin plays an important role in this process via a dual, local effect on the extracellular matrix, the cell wall, which determines cell shape. Our study reveals that auxin not only causes a limited reduction in wall stiffness but also directly interferes with wall anisotropy via the regulation of cortical microtubule dynamics. We further show that to induce growth isotropy and organ outgrowth, auxin somehow interferes with the cortical microtubule-ordering activity of a network of proteins, including AUXIN BINDING PROTEIN 1 and KATANIN 1. Numerical simulations further indicate that the induced isotropy is sufficient to amplify the effects of the relatively minor changes in wall stiffness to promote organogenesis and the establishment of new growth axes in a robust manner.

## Results and Discussion

How shape is regulated in multicellular organisms is a key question in developmental biology. Plants provide a system of choice to explore this issue because of their continuous, life-spanning organogenesis. By forming a system of

branched axes, plants explore and occupy space in an efficient manner. This mode of growth largely depends on shoot apical meristems (SAMs), groups of undifferentiated cells that initiate all the aerial organs of the plant [1, 2]. To generate a branched structure, the SAMs have to form new axes in new directions. The maintenance of existing growth directions and the definition of new ones are, therefore, fundamental to the establishment of plant architecture.

The generation of lateral organs at the SAM depends on the hormone auxin (IAA). At the SAM epidermis, auxin is actively transported via the PIN-FORMED1 (PIN1) efflux carrier, concentrating the hormone at precise locations, where it triggers the formation of new primordia [3–6]. It is, however, unclear how auxin triggers the changes in the initiation of new growth axes.

In plants, the directions and rates of growth largely depend on the mechanical properties of the polysaccharidic cell wall that glues cells together, preventing cell sliding and migration. It is widely accepted that the irreversible, plastic yielding of the wall to the internal turgor pressure, through wall synthesis and remodeling, controls cell expansion. Previous studies have pointed to the importance of wall remodeling and elasticity at the SAM, via wall-loosening proteins [7, 8]. Auxin is thought to promote primordia formation, at least in part, through this process [1, 2]. However, this represents a rather one-sided view of the contribution of wall mechanics to organogenesis. Here, we focus our attention on another essential aspect of the wall, i.e., its mechanical anisotropy. The anisotropic properties of the cell wall are mainly determined by the orientation of the rigid cellulose microfibrils [9, 10]. This orientation is controlled by cortical microtubules (CMTs), which guide the cellulose synthase complexes [11–13]. As a consequence, the mechanical anisotropy of the wall can be inferred from CMT organization. When auxin transport is genetically or chemically inhibited, as in *pin1* mutants or after treatment with Naphtylphthalamic acid (NPA), plants are unable to form organs, resulting in pin-shaped apices that only grow along the vertical axis [3, 14]. In these apices, ordered circumferential CMT patterns at the periphery of the SAM force the tissue to grow in one main direction [15]. To induce a lateral organ, auxin must somehow break the anisotropic growth of the stem, but how this occurs is not yet understood.

To investigate this issue, we set up an experimental system to induce organs from an anisotropic pin-shaped SAM: *Arabidopsis thaliana* plants were grown on NPA-containing medium to prevent the formation of flowers and subsequently were treated with IAA to induce the outgrowth of a ring-shaped structure, displaying organ primordium identity, around the SAM (Figures S1A and S1B available online). We used this system to monitor the behavior of the microtubule marker 35S::GFP-MBD during auxin-induced organogenesis. We limited our analysis to the outer layer of the SAM, which is considered rate limiting for growth [16–18]. As previously shown [15], CMTs were organized in supracellular, circumferential alignments at the periphery of pin-shaped SAMs (Figure S1C). Auxin treatments led to the disorganization of CMTs across the SAM within 24 hr, resulting in a complete loss of circumferential CMT anisotropy (Figures 1A–1E;

\*Correspondence: [massimiliano.sassi@ens-lyon.fr](mailto:massimiliano.sassi@ens-lyon.fr) (M.S.), [jan.traas@ens-lyon.fr](mailto:jan.traas@ens-lyon.fr) (J.T.)

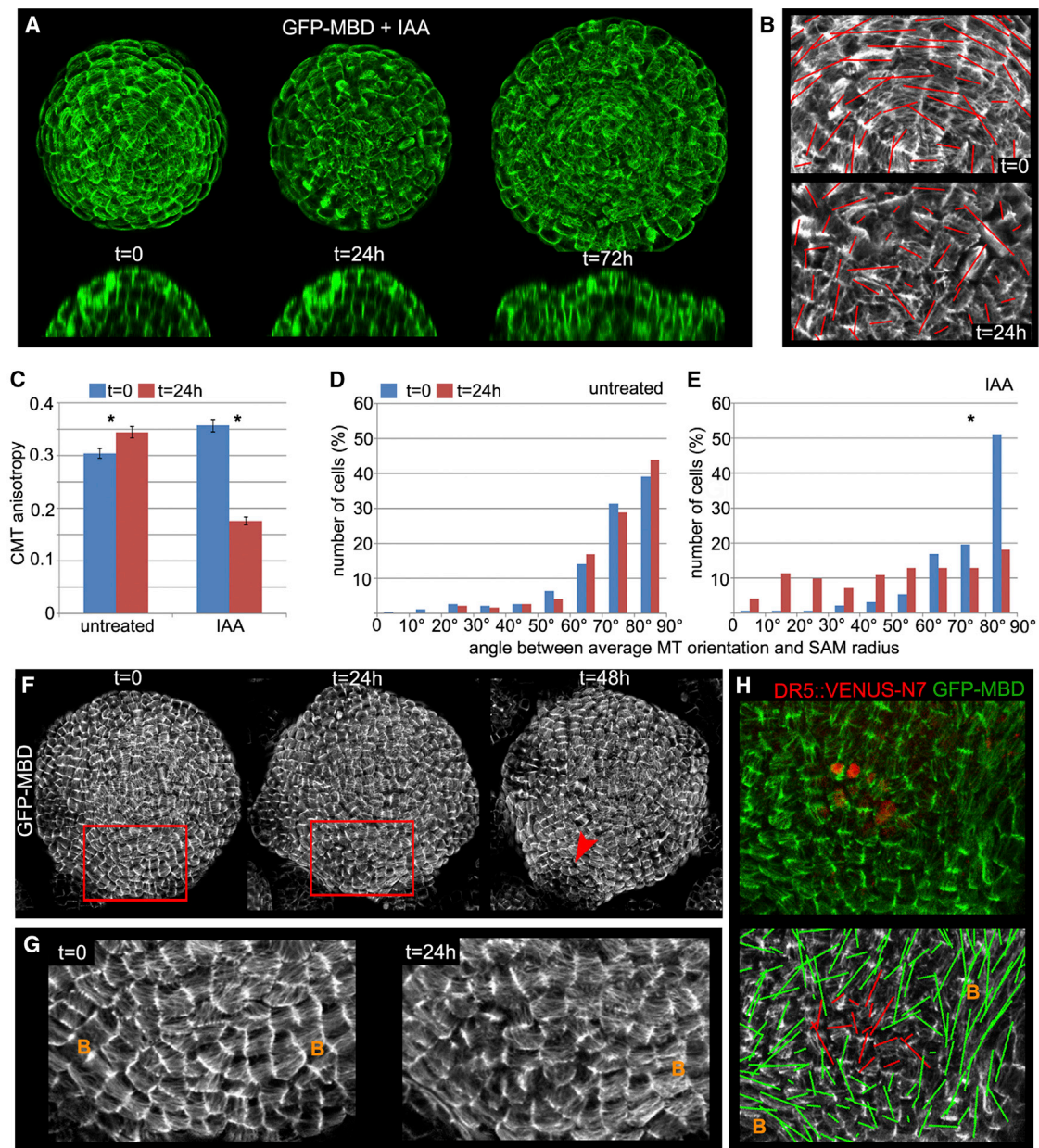


**Figure 1. Auxin Disrupts CMT Organization at the SAM before Organ Outgrowth**

(A) Surface projections of a GFP-MBD SAM treated with IAA to induce organ formation. The full time course is shown in [Figure S1](#).

(B) Details of CMT organization of the SAM shown in (A) before ( $t = 0$ ) and 24 hr after IAA application. The red bars represent the output of the CMT measurements (see [Supplemental Experimental Procedures](#)). The direction and the length of the bars indicate, respectively, the average orientation and anisotropy of CMTs in each cell.

(C) Quantification of CMT anisotropy in untreated and IAA-treated SAMs, analyzed at the indicated times. Error bars show SEM.  $*p < 0.01$ .

(D and E) Quantification of the supracellular organization of CMTs in untreated (D) and IAA-treated (E) SAMs, analyzed at the indicated times. The graphs show the distribution of the angles between the average CMT orientation and the radius of the SAM measured in each cell.  $*p < 0.01$ .

(F and G) Time course imaging of a GFP-MBD SAM grown in vivo showing the formation of a primordium (arrowhead) at  $t = 48$  hr (F). In (G), details of CMT organization in the regions highlighted in red at  $t = 0$  and  $t = 24$  hr in (F) are shown. B, boundaries.

(H) Spatiotemporal overlap between CMT disorganization and peaks of auxin activity at the SAM. Upper panel: CMT patterns, visualized by GFP-MBD (green), at the incipient primordium, marked by DR5::VENUS-N7 (red). Lower panel: Merge of the CMT measurements and the GFP-MBD channel (grayscale). DR5-expressing cells (marked in red) are enclosed in a discrete region displaying disorganized CMT patterns compared to highly anisotropic boundaries. B, boundaries.

[Figure S1D](#)). CMT disorganization preceded the formation of outgrowths, only visible 72 hr after the initial auxin application ([Figure 1A](#); [Figure S1D](#)). Discrete regions displaying disorganized CMTs were also observed in the SAM of soil-grown

plants, i.e., in the presence of an active auxin transport and preexisting lateral organs. These regions displayed substantially different GFP-MBD patterns, compared to highly anisotropic organ boundaries [15], and produced visible organ

**Growth Anisotropy Regulates SAM Organogenesis**

3

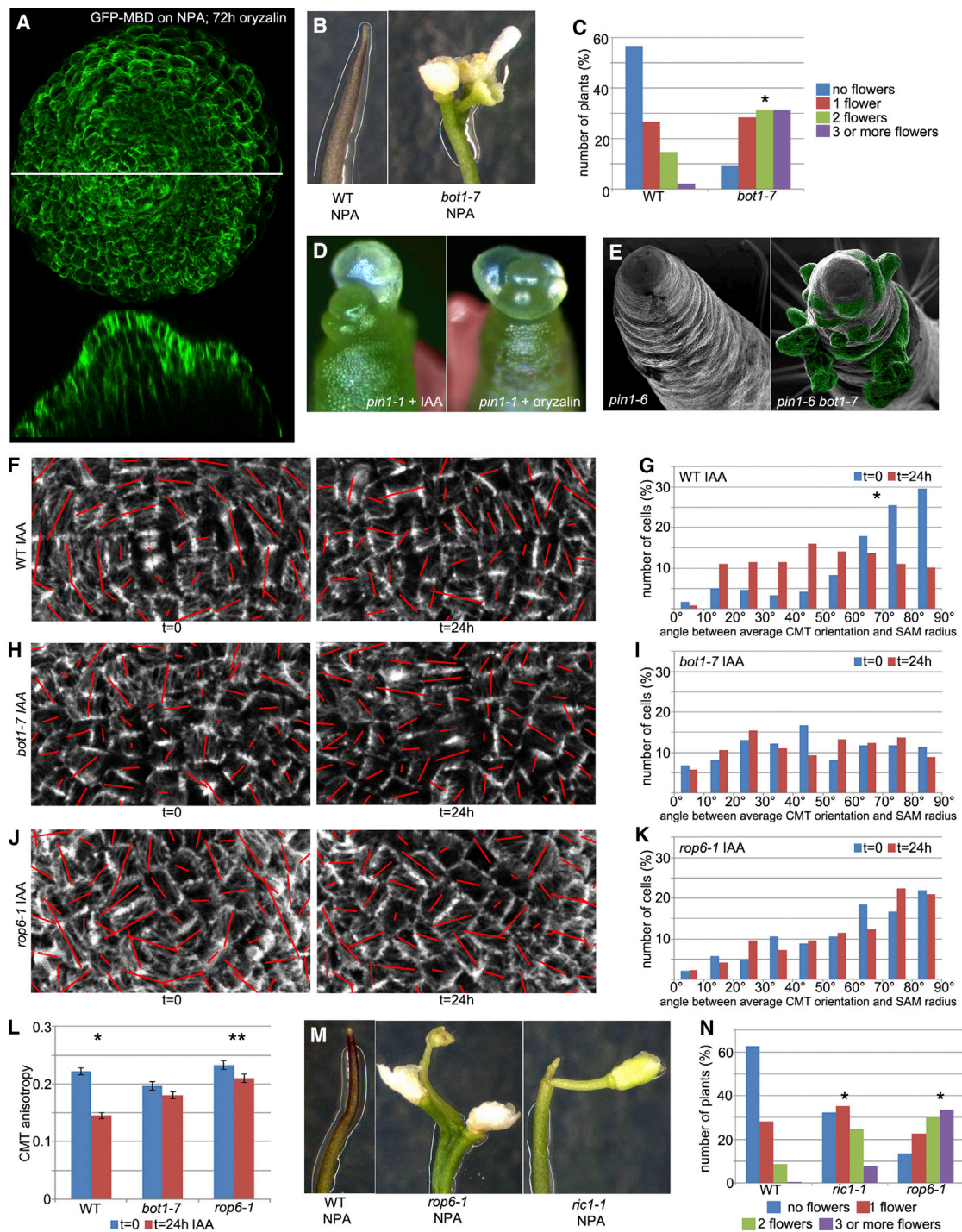


**Figure 2. Loss of CMT Anisotropy Promotes SAM Organogenesis in the Absence of Auxin Transport**

(A) Local oryzalin applications in lanolin paste disrupt CMT organization and promote the formation of a circular outgrowth after 72 hr in NPA-induced pins (upper image). Lower image: orthogonal projection drawn along the white line.  
 (B and C) *bot1-7* mutation promotes organ formation in absence of auxin transport. (B) Shoot apices of NPA-grown WT and a *bot1-7* are shown. Note spontaneous flower formation in *bot1-7*. (C) Quantification of phenotypes shown in (B). \* $p < 0.01$ .  
 (D) Local oryzalin applications promote the formation of a circular outgrowth in *pin1-1* SAMs after 96 hr (right). Local applications of IAA were used as positive controls (left). Lanolin is pseudocolored in red.  
 (E) *bot1-7* mutation promotes the formation of several outgrowths (pseudocolored in green; right) in an otherwise naked *pin1-6* background (left).  
 (F and G) CMT organization in SAM cells of WT before ( $t = 0$ ) or 24 hr after IAA treatment. (F) Details of GFP-MBD organization are shown. (G) Supracellular organization of CMTs is shown. \* $p < 0.01$ .  
 (H and I) CMT organization in SAM cells of *bot1-7* before ( $t = 0$ ) or 24 hr after IAA treatment. (H) Details of GFP-MBD organization are shown. (I) Supracellular organization of CMTs is shown.

(legend continued on next page)

primordia 24 hr later (Figures 1F and 1G). Disorganized GFP-MBD patterns at the SAM correlated in time and space with peaks of high auxin activity inferred from the auxin-signaling reporter DR5::VENUS-N7, the earliest marker of incipient primordia identified to date [5] (Figure 1H). These results suggest that, in vivo, changes in CMT anisotropy coincide with auxin maxima and precede organ outgrowth at the SAM.

We next investigated whether CMT disorganization could be instrumental in the formation of lateral outgrowths. To this end, we used the microtubule-depolymerizing drug oryzalin to alter CMT dynamics at the SAM of NPA-induced pins. Local applications of oryzalin in lanolin paste on naked meristems caused CMT disorganization, leading to ring-like outgrowths (Figure 2A). We next altered CMT dynamics by using the *botero1-7* (*bot1-7*) allele of *KATANIN1* (*KTN1*). *KTN1* encodes a microtubule-severing protein that promotes bundling and ordered CMT patterns [19–21]. *KTN1* is active in the SAM, where it contributes to the formation of anisotropic CMT arrays [22]. *bot1-7* mutants grown on NPA displayed spontaneous outgrowths that were preceded by localized CMT disorganization (Figure S2A). Indeed, more than 90% of the *bot1-7* population ( $n = 183$ ) produced flowers (compared to ~40% in the wild-type [WT] population,  $n = 143$ ) (Figures 2B and 2C) on NPA.

Moreover, we used the *pin1* mutant to perturb auxin distribution, and we tested whether oryzalin and the *bot1-7* mutation could rescue its defective organogenesis. We found that 63.4% ( $n = 41$ ) of *pin1-1* SAMs treated locally with oryzalin developed outgrowths after 4 days (Figure 2D). Similar frequencies were obtained when *pin1-1* SAMs were locally treated with IAA (66.6%;  $n = 33$ ) (Figure 2D). Likewise, the majority of *pin1-6 bot1-7* double mutants (77.8%;  $n = 14$ ) displayed a high number of lateral outgrowths around the SAM, whereas high numbers are only rarely (10.0%;  $n = 10$ ) observed in *pin1-6* single mutants (Figure 2E). Together, these results point to a causal link between loss of CMT anisotropy and organogenesis.

In auxin transport-depleted backgrounds, the *bot1-7* mutation replicates the effect of auxin treatments on CMT organization and organ initiation. Relevantly, auxin treatments were not able to further affect CMTs in *bot1-7* SAMs (Figures 2F, 2G, and 2L; Figure S2B). This suggests that (1) at low auxin concentrations, *KTN1* leads to the formation of a pin, and (2) *KTN1* is no longer able to maintain a pin in the presence of high auxin levels. It was recently proposed that auxin regulates *KTN1* function through RHO-LIKE GTPASE FROM PLANTS 6 (*ROP6*) and its effector ROP-INTERACTIVE CRIB MOTIF-CONTAINING PROTEIN 1 (*RIC1*), which binds to and activates *KTN1* [23–26]. Both *ROP6* and *RIC1* were expressed at the shoot apex, albeit at different levels (Figure S2C), and their corresponding mutants displayed a significant increase in organ formation on NPA (*rop6-1*: 86%,  $n = 146$ ; *ric1-1*: 68%,  $n = 210$ ) compared to the WT (36%,  $n = 174$ ) (Figures 2M and 2N). CMT responses to auxin treatments were impaired in *rop6-1* because no changes in CMT organization at the tissue level and only a minor decrease of cellular CMT anisotropy were observed (Figures 2J, 2K, and 2L; Figure S2B).

The *ROP6*-dependent regulation of CMT organization has been associated with the extracellular auxin receptor AUXIN BINDING PROTEIN 1 (*ABP1*) signaling [25–27]. *ABP1* is expressed at the SAM (Figure S2C) [28]; therefore, we investigated whether it could be involved in the regulation of CMT organization at the SAM. Because *ABP1* knockout mutants are embryo lethal [29, 30], we first employed the viable *abp1-5* allele, containing a point mutation in the auxin-binding pocket that reduces the affinity to auxin [25, 31]. Compared to the WT, *abp1-5* mutants displayed relatively subtle promotion of organ formation on NPA (Figures 3A and 3B). Indeed, *abp1-5* SAMs displayed only minor alterations in the circumferential CMT organization (Figures 3E and 3F,  $t = 0$ ; Figure S3A,  $t = 0$ ) and were still able to respond to auxin treatments, albeit to a lesser extent compared to the WT (Figures 3C–3F and 3I; Figure S3A). Consequently, auxin-induced organ initiation was severely delayed in *abp1-5* SAMs compared to the WT (Figures S3B and S3C). To gain insights into *ABP1* function in the regulation of CMT organization and SAM organogenesis, we generated a transheterozygous mutant bearing one copy of the auxin-insensitive *abp1-5* and one copy of the embryo-lethal null *abp1-1s* allele [30]. The resulting *abp1-1s/abp1-5* was viable and displayed enhanced organ formation and more-random CMT organization compared to the parental *abp1-5* on NPA (Figures 3A and 3B; Figure S3D). CMTs in *abp1-1s/abp1-5* SAMs were completely insensitive to auxin treatments for both cell and tissue responses (Figures 3G, 3H, and 3I; Figure S3A), similar to *bot1-7* mutants. This suggests that *ABP1* and *KTN1* act in a similar manner to regulate CMT organization and SAM organogenesis. Coherently, *bot1-7 abp1-5* mutants displayed organ initiation phenotypes on NPA, similar to those of the parental *bot1-7* (Figure S3E), and no novel additive phenotypes were observed. This is in line with the hypothesis that *ABP1* and *KTN1* act in the same pathway, as previously reported in other systems [25–27], although further experiments are needed to clarify this issue.

Together, our results suggest that in the absence of auxin accumulation, a network of interacting proteins, including *KTN1*, *ROP6/RIC1*, and *ABP1*, keep microtubular arrays at the SAM in an anisotropic state. This is sufficient to inhibit spontaneous lateral outgrowth, leading to the formation of a pin-shaped stem. In the presence of high auxin levels, these molecules are no longer able to maintain CMT anisotropy, which induces a shift toward isotropic cell walls. As a result, organ outgrowth is promoted.

As discussed above, previous studies have suggested a role of cell wall remodeling and extensibility in SAM organogenesis [7, 8]. In addition, there are indications that inner layers of the meristem loosen their walls just before organ outgrowth, leaving the outer layer as the main growth-limiting factor [32, 33]. This is consistent with the observation that the outer layer has thicker cell walls than the inner layers [18]. Altogether, this implies that organogenesis results from the modulation of both cell wall stiffness and anisotropy. Why would two different layers of regulation be required? To explore this question, we used an in silico model in the form of a virtual

(J and K) CMT organization in SAM cells of *rop6-1* before ( $t = 0$ ) or 24 hr after IAA treatment. (J) Details of GFP-MBD organization are shown. (K) Supracellular organization of CMTs is shown.

(L) Quantification of CMT anisotropy in the SAM cells of WT, *bot1-7*, and *rop6-1* before ( $t = 0$ ) and 24 hr after IAA treatment. \* $p < 0.01$ ; \*\* $p < 0.05$ . Error bars show SEM.

(M and N) *rop6-1* and *ric1-1* promote organ formation in absence of auxin transport. (M) Shoot apices of NPA-grown WT, *rop6-1*, and *ric1-1* plants are shown.

(P) Quantification of phenotypes shown in (N). \* $p < 0.01$ .

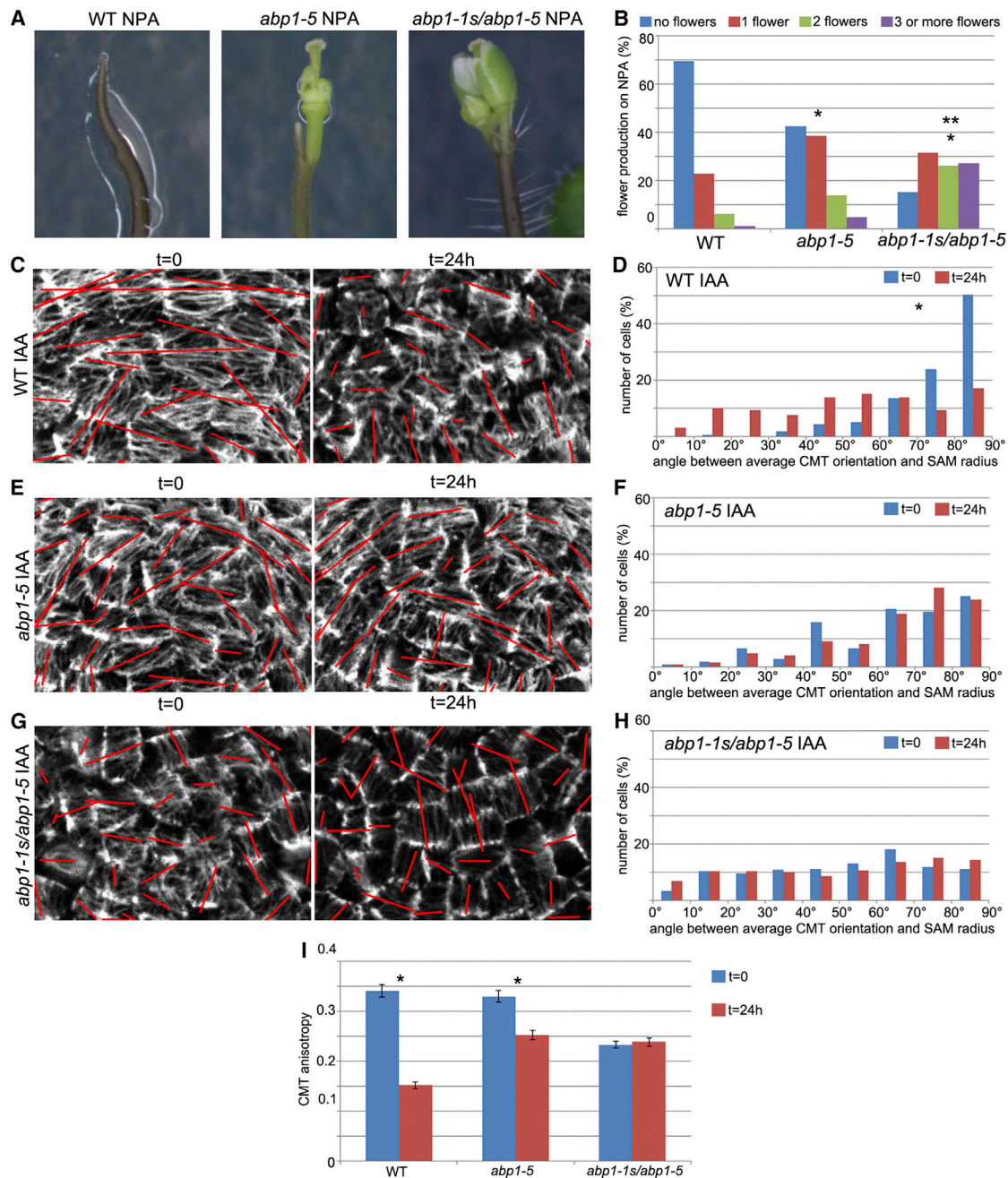


Figure 3. ABP1 Regulates Organ Formation and Auxin Responsiveness of CMTs at the SAM

(A and B) Mutations in ABP1 promote organ formation in absence of auxin transport. (A) Shoot apices of NPA-grown WT (n = 240), *abp1-5* (n = 204), and *abp1-1s/abp1-5* (n = 92) are shown. (B) Quantification of the phenotypes shown in (A). Mutant versus WT: \*p < 0.01; *abp1-5* versus *abp1-1s/abp1-5*: \*\*p < 0.01.

(C and D) CMT organization in SAM cells of WT before (t = 0) or 24 hr after IAA treatment. (C) Details of GFP-MBD organization are shown. (D) Supracellular organization of CMTs is shown. \*p < 0.01.

(E and F) CMT organization in SAM cells of *abp1-5* before (t = 0) or 24 hr after IAA treatment. (E) Details of GFP-MBD organization are shown. (F) Supracellular organization of CMTs is shown.

(G and H) CMT organization in SAM cells of *abp1-1s/abp1-5* before (t = 0) or 24 hr after IAA treatment. (E) Details of GFP-MBD organization are shown. (F) Supracellular organization of CMTs is shown.

(I) Quantification of CMT anisotropy in SAMs of WT, *abp1-5*, and *abp1-1s/abp1-5* before (t = 0) and 24 hr after IAA treatment. Error bars show SEM. \*p < 0.01.

3D meristematic dome in which the mechanical and geometrical parameters can be set in each cell (Figure 4A). In the model, virtual genes can act on wall elasticity, turgor pressure, the yield threshold above which synthesis occurs, and the

synthesis rate itself. Based on the microtubule patterns observed in the pin-like SAM in vivo, anisotropic growth was imposed on the peripheral cells of the virtual meristems. The summit of the dome was kept isotropic and slow growing to

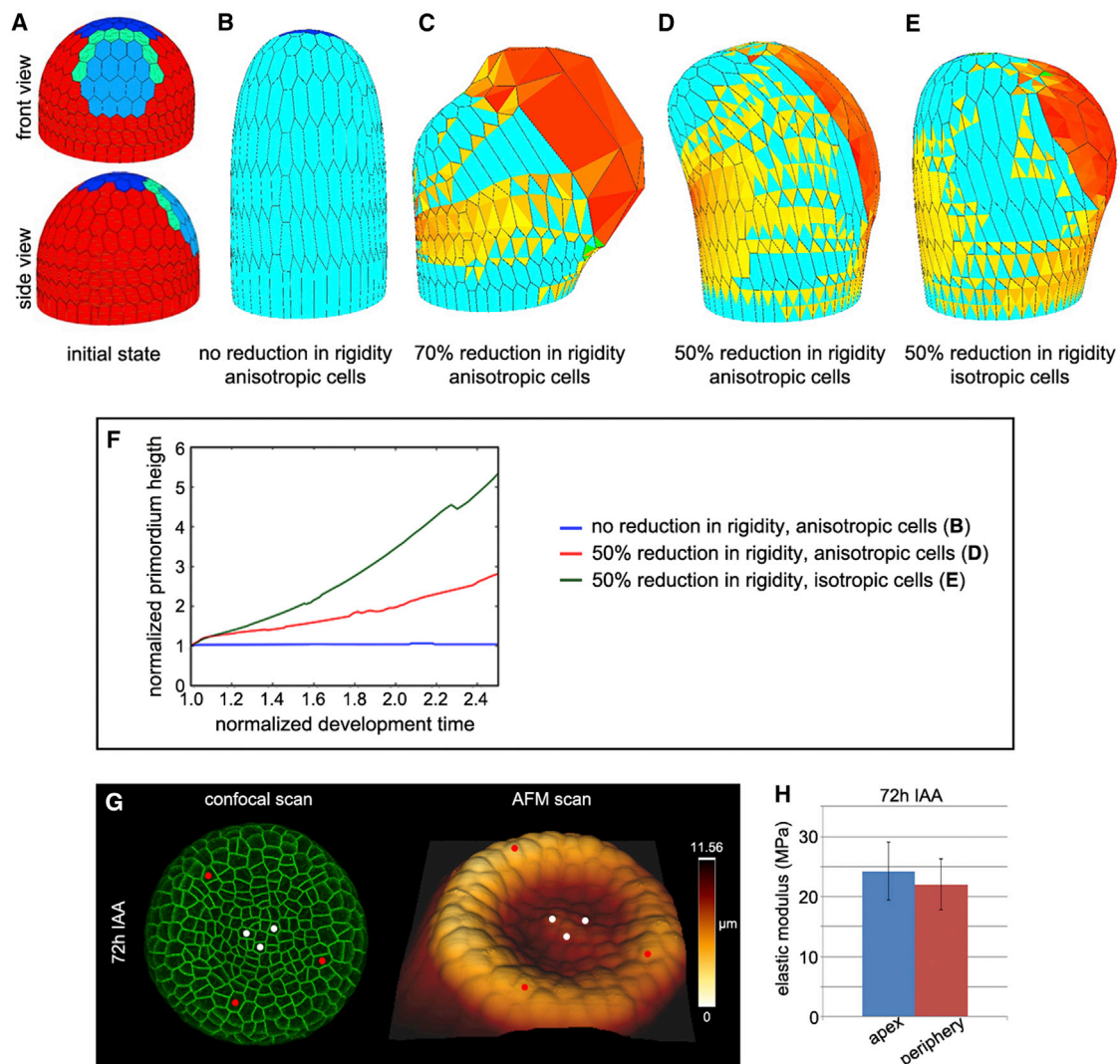


**Figure 4. Loss of CMT Anisotropy Amplifies the Effect of Minor Reductions in Cell Wall Rigidity to Induce Organ Outgrowth at the SAM**

(A) Front and side views of the virtual meristem in its initial state showing the subdivision in different zones: dark blue indicates central zone; red indicates peripheral zone; light blue indicates primordium; and turquoise indicates frontier.

(B) Endpoint of a simulation showing the development of a pin-like structure with constant wall rigidity and anisotropic cells at the primordium. See also [Movie S1](#).

(C) Endpoint of a simulation showing the development of an outgrowth following a 70% reduction in wall rigidity with anisotropic cells at the primordium. See also [Movie S2](#).

(D) Endpoint of a simulation showing the bending of the virtual meristem following a 50% reduction in wall rigidity with anisotropic cells at the primordium. See also [Movie S3](#).

(E) Endpoint of a simulation showing the development of an outgrowth following a 50% reduction in wall rigidity when primordium cells are isotropic. See also [Movie S4](#).

(F) A 50% reduction in wall rigidity coupled to isotropic cells (green) displays increased growth rates compared to the same reduction in wall rigidity coupled to anisotropic cells (red). Growth rates are constant when cell wall rigidity is unchanged and cells are anisotropic (blue).

(G) Confocal and AFM surface 3D reconstructions of the same 35S::GFP-LTI6b NPA pin, 72 hr after the beginning of the IAA treatment. Colored dots mark the same cells to facilitate the comparison of the two images. The color scale represents the height of the AFM image.

(H) Histogram depicting the average elastic modulus in apical and peripheral cells of eight SAMs measured by AFM scans 72 hr after the beginning of the IAA treatment. See also [Figure S4](#). Error bars show SEM.

represent the central zone of the SAM [15]. The pressure in this virtual stem was not sufficient to reach the yielding threshold in the circumferential direction, leading to a cylindrical stem with a constant diameter, as observed in pin-like apices in vivo ([Figure 4B](#); [Movie S1](#)). To investigate the potential of wall loosening, we imposed changes in wall stiffness, without changing growth anisotropy, in a small group of peripheral primordium cells in the model. Relevantly, an outgrowth was generated

only after a 70% reduction in wall rigidity ([Figure 4C](#); [Movie S2](#)). When the reduction was set to 50%, the meristem bent to the opposite side of the loosened cells, and no clear bulge was obtained ([Figure 4D](#); [Movie S3](#)). This made us wonder about the actual extent of cell wall loosening during organogenesis in vivo. To investigate this issue, we employed atomic force microscopy (AFM) to quantify locally (in the range of 100 nm in depth) the mechanical properties of the outer wall

[34]. Using this protocol on auxin-treated SAMs, we observed variable changes in the elastic modulus, with a tendency of the outgrowth to become slightly softer than the apex (Figures 4G and 4H). Such changes did not exceed 30% (Figure S4), indicating that major reductions in the outer wall rigidity do not occur during organ initiation.

We therefore performed a series of additional simulations, this time combining a limited reduction in wall stiffness with a shift to isotropy in the primordium. This led to the formation of an outgrowth at the flank of the virtual meristem (Figure 4E; Movie S4). Relevantly, the combination of limited loosening and isotropy led to increased primordium growth rates compared to the simulations using limited loosening alone (Figure 4F). Our theoretical analysis therefore suggests that the anisotropy-to-isotropy shift could promote organ formation by amplifying the effect of relatively minor reductions in the outer wall rigidity at the SAM.

In conclusion, we show that at the SAM periphery, auxin interferes with CMT anisotropy, which normally forces the apical tissues to develop into a single cylindrical axis. By locally counteracting the polarizing effect of these circumferential CMT arrays, auxin generates new axes for lateral organ outgrowth without perturbing the vertical growth of the stem, allowing the plant to explore efficiently new directions in space.

#### Supplemental Information

Supplemental Information includes Supplemental Experimental Procedures, four figures, and four movies and can be found with this article online at <http://dx.doi.org/10.1016/j.cub.2014.08.036>.

#### Author Contributions

M.S. and J.T. designed the study. M.S., C.C., and U.A. performed the biological experiments. G.C. and O.A. carried out the AFM analysis. O.A., F.B., B.G., and C.G. carried out numerical simulations. X.C., J.F., T.V., and O.H. provided materials/reagents. M.S. and J.T. analyzed the data and wrote the manuscript, with contributions from all the authors.

#### Acknowledgments

This work was funded by grants from EraSysBio+ (iSAM) and ERC (Morphodynamics). We thank Dolf Weijers (Wageningen University) and Zhenbiao Yang (Riverside University) for generously providing seeds. We thank all the member of the J.T. laboratory for helpful discussions and Arezki Boudaoud and Roberta Galletti for helpful discussions and critical reading of the manuscript.

Received: January 6, 2014

Revised: July 3, 2014

Accepted: August 15, 2014

Published: September 25, 2014

#### References

- Murray, J.A.H., Jones, A., Godin, C., and Traas, J. (2012). Systems analysis of shoot apical meristem growth and development: integrating hormonal and mechanical signaling. *Plant Cell* 24, 3907–3919.
- Sassi, M., and Vernoux, T. (2013). Auxin and self-organization at the shoot apical meristem. *J. Exp. Bot.* 64, 2579–2592.
- Reinhardt, D., Mandel, T., and Kuhlemeier, C. (2000). Auxin regulates the initiation and radial position of plant lateral organs. *Plant Cell* 12, 507–518.
- Reinhardt, D., Pesce, E.-R., Stieger, P., Mandel, T., Baltensperger, K., Bennett, M., Traas, J., Friml, J., and Kuhlemeier, C. (2003). Regulation of phyllotaxis by polar auxin transport. *Nature* 426, 255–260.
- Heisler, M.G., Ohno, C., Das, P., Sieber, P., Reddy, G.V., Long, J.A., and Meyerowitz, E.M. (2005). Patterns of auxin transport and gene expression during primordium development revealed by live imaging of the *Arabidopsis* inflorescence meristem. *Curr. Biol.* 15, 1899–1911.
- Benková, E., Michniewicz, M., Sauer, M., Teichmann, T., Seifertová, D., Jürgens, G., and Friml, J. (2003). Local, efflux-dependent auxin gradients as a common module for plant organ formation. *Cell* 115, 591–602.
- Fleming, A.J., McQueen-Mason, S., Mandel, T., and Kuhlemeier, C. (1997). Induction of leaf primordia by the cell wall protein expansin. *Science* 276, 1415–1418.
- Peaucelle, A., Louvet, R., Johansen, J.N., Höfte, H., Laufs, P., Pelloux, J., and Mouille, G. (2008). *Arabidopsis* phyllotaxis is controlled by the methyl-esterification status of cell-wall pectins. *Curr. Biol.* 18, 1943–1948.
- Somerville, C., Bauer, S., Brininstool, G., Facette, M., Hamann, T., Milne, J., Osborne, E., Paredez, A., Persson, S., Raab, T., et al. (2004). Toward a systems approach to understanding plant cell walls. *Science* 306, 2206–2211.
- Cosgrove, D.J. (2005). Growth of the plant cell wall. *Nat. Rev. Mol. Cell Biol.* 6, 850–861.
- Paredez, A.R., Somerville, C.R., and Ehrhardt, D.W. (2006). Visualization of cellulose synthase demonstrates functional association with microtubules. *Science* 312, 1491–1495.
- Gutierrez, R., Lindeboom, J.J., Paredez, A.R., Emons, A.M.C., and Ehrhardt, D.W. (2009). *Arabidopsis* cortical microtubules position cellulose synthase delivery to the plasma membrane and interact with cellulose synthase trafficking compartments. *Nat. Cell Biol.* 11, 797–806.
- Bringmann, M., Li, E., Sampathkumar, A., Kocabek, T., Hauser, M.-T., and Persson, S. (2012). POM-POM2/cellulose synthase interacting1 is essential for the functional association of cellulose synthase and microtubules in *Arabidopsis*. *Plant Cell* 24, 163–177.
- Okada, K., Ueda, J., Komaki, M.K., Bell, C.J., and Shimura, Y. (1991). Requirement of the auxin polar transport system in early stages of *Arabidopsis* floral bud formation. *Plant Cell* 3, 677–684.
- Hamant, O., Heisler, M.G., Jönsson, H., Krupinski, P., Uyttewaal, M., Bokov, P., Corson, F., Sahlín, P., Boudaoud, A., Meyerowitz, E.M., et al. (2008). Developmental patterning by mechanical signals in *Arabidopsis*. *Science* 322, 1650–1655.
- Savaldi-Goldstein, S., Peto, C., and Chory, J. (2007). The epidermis both drives and restricts plant shoot growth. *Nature* 446, 199–202.
- Reinhardt, D., Frenz, M., Mandel, T., and Kuhlemeier, C. (2003). Microsurgical and laser ablation analysis of interactions between the zones and layers of the tomato shoot apical meristem. *Development* 130, 4073–4083.
- Kierzkowski, D., Nakayama, N., Routier-Kierzkowska, A.-L., Weber, A., Bayer, E., Schorderet, M., Reinhardt, D., Kuhlemeier, C., and Smith, R.S. (2012). Elastic domains regulate growth and organogenesis in the plant shoot apical meristem. *Science* 335, 1096–1099.
- Bichet, A., Desnos, T., Turner, S., Grandjean, O., and Höfte, H. (2001). BOTERO1 is required for normal orientation of cortical microtubules and anisotropic cell expansion in *Arabidopsis*. *Plant J.* 25, 137–148.
- Burk, D.H., and Ye, Z.H. (2002). Alteration of oriented deposition of cellulose microfibrils by mutation of a katanin-like microtubule-severing protein. *Plant Cell* 14, 2145–2160.
- Stoppin-Mellet, V., Gaillard, J., and Vantard, M. (2006). Katanin's severing activity favors bundling of cortical microtubules in plants. *Plant J.* 46, 1009–1017.
- Uyttewaal, M., Burian, A., Alim, K., Landrein, B., Borowska-Wykręt, D., Dedieu, A., Peaucelle, A., Ludynia, M., Traas, J., Boudaoud, A., et al. (2012). Mechanical stress acts via katanin to amplify differences in growth rate between adjacent cells in *Arabidopsis*. *Cell* 149, 439–451.
- Fu, Y., Gu, Y., Zheng, Z., Wasteneys, G., and Yang, Z. (2005). *Arabidopsis* interdigitating cell growth requires two antagonistic pathways with opposing action on cell morphogenesis. *Cell* 120, 687–700.
- Fu, Y., Xu, T., Zhu, L., Wen, M., and Yang, Z. (2009). A ROP GTPase signaling pathway controls cortical microtubule ordering and cell expansion in *Arabidopsis*. *Curr. Biol.* 19, 1827–1832.
- Xu, T., Wen, M., Nagawa, S., Fu, Y., Chen, J.-G., Wu, M.-J., Perrot-Rechenmann, C., Friml, J., Jones, A.M., and Yang, Z. (2010). Cell surface- and rho GTPase-based auxin signaling controls cellular interdigitation in *Arabidopsis*. *Cell* 143, 99–110.
- Lin, D., Cao, L., Zhou, Z., Zhu, L., Ehrhardt, D., Yang, Z., and Fu, Y. (2013). Rho GTPase signaling activates microtubule severing to promote microtubule ordering in *Arabidopsis*. *Curr. Biol.* 23, 290–297.



27. Xu, T., Dai, N., Chen, J., Nagawa, S., Cao, M., Li, H., Zhou, Z., Chen, X., De Rycke, R., Rakusová, H., et al. (2014). Cell surface ABP1-TMK auxin-sensing complex activates ROP GTPase signaling. *Science* **343**, 1025–1028.
28. Braun, N., Wyrzykowska, J., Muller, P., David, K., Couch, D., Perrot-Rechenmann, C., and Fleming, A.J. (2008). Conditional repression of AUXIN BINDING PROTEIN1 reveals that it coordinates cell division and cell expansion during postembryonic shoot development in *Arabidopsis* and tobacco. *Plant Cell* **20**, 2746–2762.
29. Chen, J.G., Ullah, H., Young, J.C., Sussman, M.R., and Jones, A.M. (2001). ABP1 is required for organized cell elongation and division in *Arabidopsis* embryogenesis. *Genes Dev.* **15**, 902–911.
30. Tzafrir, I., Pena-Muralla, R., Dickerman, A., Berg, M., Rogers, R., Hutchens, S., Sweeney, T.C., McElver, J., Aux, G., Patton, D., and Meinke, D. (2004). Identification of genes required for embryo development in *Arabidopsis*. *Plant Physiol.* **135**, 1206–1220.
31. Robert, S., Kleine-Vehn, J., Barbez, E., Sauer, M., Paciorek, T., Baster, P., Vanneste, S., Zhang, J., Simon, S., Čovanová, M., et al. (2010). ABP1 mediates auxin inhibition of clathrin-dependent endocytosis in *Arabidopsis*. *Cell* **143**, 111–121.
32. Peaucelle, A., Braybrook, S.A., Le Guillou, L., Bron, E., Kuhlemeier, C., and Höfte, H. (2011). Pectin-induced changes in cell wall mechanics underlie organ initiation in *Arabidopsis*. *Curr. Biol.* **21**, 1720–1726.
33. Braybrook, S.A., and Peaucelle, A. (2013). Mechano-chemical aspects of organ formation in *Arabidopsis thaliana*: the relationship between auxin and pectin. *PLoS ONE* **8**, e57813.
34. Milani, P., Gholamirad, M., Traas, J., Arnéodo, A., Boudaoud, A., Argoul, F., and Hamant, O. (2011). In vivo analysis of local wall stiffness at the shoot apical meristem in *Arabidopsis* using atomic force microscopy. *Plant J.* **67**, 1116–1123.